Controlled Thiolate Coordination and Redox Chemistry: Synthesis, Structure, Axial-Binding, and Electrochemistry of Dinickel(II) Dithiolate Macrocyclic Complexes

Sally Brooker,*[a] Paul D. Croucher,[a] Tony C. Davidson,[a] Geoffrey S. Dunbar,[a] Corina U. Beck,[b] and S. Subramanian[c]

Keywords: Macrocycles / Nickel / Redox chemistry / Schiff bases / S ligands

A single crystal X-ray analysis of $[Ni_2L1](ClO_4)_2 \cdot MeCN \cdot 1/4\ H_2O$, **1a** [formed directly from a mixture of nickel(II) template ions, 2,6-diformyl-4-methyl-thiophenolate, and 1,4-diaminobutane] reveals that the nickel(II) ions are in square-planar N_2S_2 environments and that the four "bowed" dinickel macrocycles in the asymmetric unit pack around a single central perchlorate template ion encapsulating it to form "star" clusters of stoichiometry $\{[Ni_2L1]_4(ClO_4)\}^{7+}$. These "stars" stack together, via π–π-stacking interactions, to form two-dimensional sheets, which are separated from one another by layers of the remaining perchlorate anions and solvent molecules. Reduction, by $NaBH_4$, of the four imine bonds in $[Ni_2L2](ClO_4)_2$ **2a** (analogous to **1a** but formed from 1,3-diaminopropane not 1,4-diaminobutane) or $[Ni_2L2](CF_3SO_3)_2$ **2b** to amine bonds produces the corresponding tetra-amine complex, $[Ni_2L3](ClO_4)_2$ **3**. These complexes are shown to contain diamagnetic nickel(II) ions by a combination of magnetic, NMR and UV/Vis spectroscopic results. The ^1H NMR spectra of **1–3** run in $[D_3]MeNO_2$ and in $[D_3]MeCN$ are consistent with increasing axial binding ability in the order: **3** < **2** < **1**. Thiocyanate ion binding studies reveal that **1** and **2** are able to coordinate two thiocyanate ions, forming $[Ni_2L1(NCS)_2]$ **4** and $[Ni_2L2(NCS)_2]$ **5** respectively, whereas **3** does not. Single crystal X-ray analyses of complexes **4** · 2 MeCN and **5** · MeCN show that adjacent square-planar and octahedral nickel(II) ions result. Two one-electron oxidations *and* two one-electron reductions are a feature of the electrochemistry of **1–3** in MeCN: curiously, the potentials for the oxidation processes are almost invariant whereas those for the reduction processes vary as anticipated. EPR spectroscopy shows that the first one-electron reduction process and the first one-electron oxidation process are metal centred. Spectroelectrochemical studies and redox titrations indicate that a purplish-coloured complex is produced by one-electron oxidation of **2** (λ = 870 nm, ε = 1320 L mol cm^{-1}). The synthesis of a phenolate analogue, $[Ni_2L'(MeCN)_4](ClO_4)_2$ (**6**), of the thiophenolate complex **2a** is also detailed. Complex **6** undergoes two one-electron oxidations in MeCN, but, in contrast to the thiophenolate complexes **1–3**, these occur at much higher potentials. Only a single one-electron reduction process is observed and this occurs at a more negative potential than for any of **1–3**.

Introduction

There is intense interest in modelling nickel thiolate metalloprotein active sites including the [Ni,Fe] hydrogenases mixed metal active site which is responsible for catalysing the reversible oxidation of dihydrogen, $H_2 = 2\,H^+ + 2\,e^-$.[1–4] Many dinickel thiolate-bridged complexes have been reported although the number which have been fully characterised (ie. structure and physical properties including redox chemistry) is still relatively small.[5] As a result of these biologically-inspired studies much is being learnt about fundamental thiolate coordination chemistry. Gaining an understanding of the nature of the redox products of polynuclear thiolate complexes is a considerable and fascinating challenge.[6–9]

Robson and co-workers investigated the coordination chemistry of some acyclic ligands prepared from the thiolate-precursor (*S*)-(2,6-diformyl-4-methylphenyl)dimethyl thiocarbamate.[10–13] We,[14–19] and others[20–24] have subsequently prepared a range of Schiff-base macrocycles from this thiolate-precursor: most of these macrocycles can be templated by nickel(II) ions thus giving direct access to the complexes of interest. By using *macrocyclic* ligands the many problems typically encountered when working with transition metal thiolates are minimised and the resulting thiolate coordination chemistry can be explored in a relatively controlled way.[25] The investigation of the dinickel(II) thiolate macrocyclic complexes $[Ni_2Lj]X_2$ **1–3** (j = 1–3 and X = ClO_4^- for complexes **1a**, **2a**, and **3** respectively, j = 1–2 and X = $CF_3SO_3^-$ for complexes **1b** and **2b** respectively) and $[Ni_2Lj(NCS)_2]$ **4** and **5** (j = 1 for complex **4** and j = 2 for complex **5**), shown in Figure 1, is presented.

[a] Department of Chemistry, University of Otago, P. O. Box 56, Dunedin, New Zealand
Fax: (internat.) +64-3/479-7906
E-mail: sbrooker@alkali.otago.ac.nz
[b] School of Chemistry, University of Sydney, Sydney, NSW 2006, Australia
[c] Department of Chemistry, University of Victoria, Victoria, B.C., Canada

  1434–1948/00/0101–0169 $ 17.50+.50/0

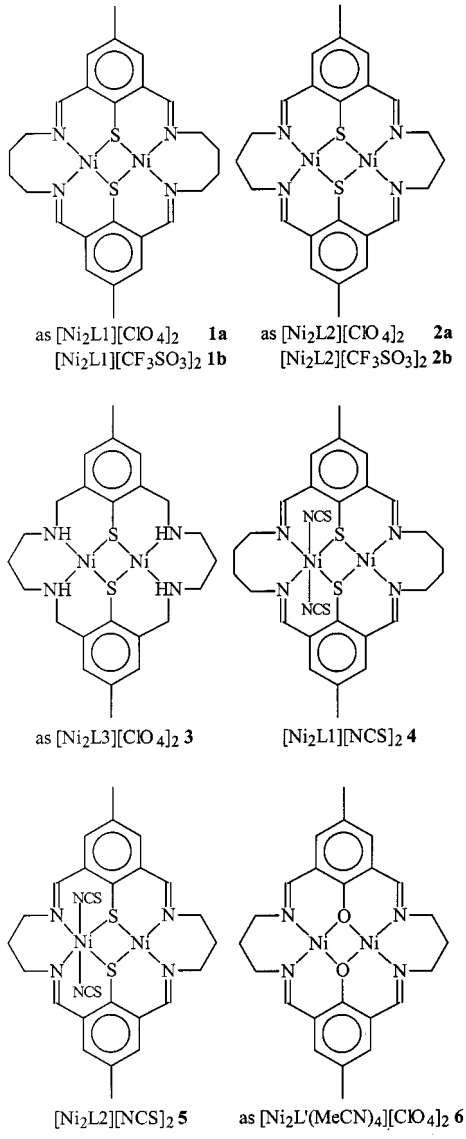

Figure 1. Macrocyclic dinickel(II) complexes **1**−**6**

Results and Discussion

Synthesis

The red complexes $[Ni_2L1](ClO_4)_2 \cdot MeCN \cdot 1/4\ H_2O$, **1a**, $[Ni_2L1](CF_3SO_3)_2 \cdot H_2O$, **1b**, and $[Ni_2L2](CF_3SO_3)_2$, **2b**, were prepared in acceptable yields. The sodium borohydride reduction of the tetra-imine analogue **2b**, to produce the red tetra-amine complex $[Ni_2L3](ClO_4)_2$ **3**, in excellent yield (80%), was carried out according to the method described by Curtis.[26] The ability of this complex to resist protonation during the acidic workup is remarkable and indicates that there is no remaining nucleophilicity associated with the bridging thiolate suphur atoms. The red-black complexes $[Ni_2L1(NCS)_2]$ **4** and $[Ni_2L2(NCS)_2]$ **5** were prepared by the addition of a solution of 2.2 equivalents of NaSCN to acetonitrile solutions of **1** and **2**, respectively. Complex **4** is obtained in excellent yield (83%) in marked contrast to **5** (19%). No change occurred on addition of 2.2 equivalents of NaSCN to a red acetonitrile solution of **3** whereas an excess of NaSCN caused the solution to turn green and deposit, over time, a green oily solid. The IR spectrum of this impure complex indicated that the nickel ions had been removed from the ligand and formed a simple salt. This was not pursued further. We found the direct preparation of the previously reported[21] phenolate complex, $[Ni_2L'(MeCN)_4](ClO_4)_2$ **6**, non-trivial. Therefore the dichloride analogue[27] was prepared and reacted with silver perchlorate[28] to give a green powder which was then recrystallised from MeCN by vapour diffusion of diethyl ether to give **6**.

In the case of the tetra-imine macrocyclic complexes **1a**, **1b**, **2b**, and **6** IR spectroscopy showed imine formation (1615, 1614, 1623, 1639 cm^{-1}, respectively) and that no unchanged carbonyl or primary amine functional groups were present. The IR spectrum of the perchlorate complex **1a** did not show bands consistent with the very small amount of lattice water present (1/4 H_2O per macrocyclic complex) whereas for the triflate complex **1b** the IR spectrum was consistent with the presence of lattice water[29] (bands were observed at 3526, 3462, and 1623 cm^{-1}) and this was subsequently confirmed by microanalysis (one H_2O per macrocyclic complex). In contrast, the triflate complex **2b** did not have these IR bands and microanalysis gave no evidence for the presence of any waters of crystallisation. The IR spectra of **4** and **5** are consistent with retention of the imine macrocycle (1628 and 1621 cm^{-1} respectively), loss of the perchlorate anions and gain of thiocyanate anions (2081 and 2075 cm^{-1}, respectively). The brown powder formed as the major by-product in the low yielding reaction to form **5** has a shoulder at ca. 1652 cm^{-1} in the IR spectrum indicating that it is a ring-opened complex. This presumably results from imine hydrolysis relieving the strain of encircling a, larger, high spin nickel(II) ion.

Satisfactory elemental analyses were obtained for all of the new complexes, $[Ni_2L1](ClO_4)_2 \cdot MeCN \cdot 1/4\ H_2O$ **1a**, $[Ni_2L1](CF_3SO_3)_2 \cdot H_2O$ **1b**, $[Ni_2L2](CF_3SO_3)_2$ **2b**, $[Ni_2L1(NCS)_2]$ **4**, $[Ni_2L2(NCS)_2]$ **5**, and $[Ni_2L'(MeCN)_4](ClO_4)_2$ **6**. The red complexes **1**−**3** were found to be diamagnetic ($\mu = 0.0$ BM in all cases) which is consistent with a square planar nickel(II) formulation. The red-black complex **4** has a magnetic moment of 2.8 BM per complex which is consistent with the presence of a single high-spin nickel(II) ion per complex.

Crystal Structures

The structures of **2a** and **3** have been reported previously.[16][19] Red crystals of **1a** suitable for X-ray crystal structure analysis were grown from acetonitrile solutions by vapour diffusion of diethyl ether. The structure determination reveals that the asymmetric unit contains *four* dinickel(II) dithiolate macrocycles which, despite lacking crystallographic symmetry, are reasonably similar to each other and form a "star" which is templated on a perchlorate ion (Figure 2, Tables 1 and 2). Each nickel atom is square

planar, as predicted, and is located within 0.05 Å of the mean plane through the N_2S_2 donors provided by the respective macrocycle. Bonds between these donors and the nickel atoms are typical for square planar nickel(II).[16][30] In each macrocycle one of the two nickel atoms interacts very weakly with the central perchlorate ion (Figure 2, Ni···O 3.34−3.36 Å). The mean planes of the two N_2S_2 donor sets within each macrocycle intersect at angles of 137.6° [for Ni(7), Ni(8)] to 140.0° [for Ni(5), Ni(6)]. In addition, each of the macrocycles is bent such that the two aromatic rings are inclined almost at right angles (84.2−97.0°) to each other. The tetrahedrally-distorted bridging-thiolate sulfur donors (Ni−S−Ni 92.3−93.6, Ni−S−C 97.4−108.4°) facilitate this folding of the macrocycles and in doing so reveal their geometrical flexibility.[31−33]

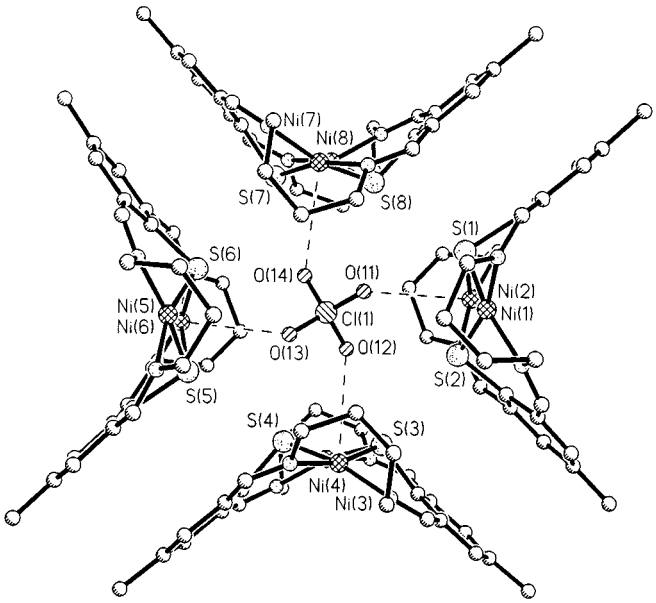

Figure 2. Perspective view of the four $[Ni_2L1]^{2+}$ cations and one of the perchlorate ions, Cl(1), in the asymmetric unit of **1a** (hydrogen atoms, solvent molecules, and remaining perchlorate ions omitted for clarity)

The folding is optimal for the formation of a large number of favourable π−π interactions both between phenyl rings within the asymmetric unit [Figure 2, pairs of π-stacked aromatic rings intersect at 7.8(7)−10.2(7)° and are 3.17(3)−3.65(1) Å apart] and between symmetry generated units [Figure 3, pairs of parallel, π-stacked aromatic rings are 3.43−3.53 Å apart]. Both edge-on ("T") and offset face-to-face π−π interactions[34] are observed and these result in the formation of sheets of dinickel macrocyclic cations, between which lie layers of counter ions and solvent molecules [with the exception of perchlorate Cl(1) which is at the centre of the four macrocycles in the asymmetric unit (Figure 2)].

Differences in the coordination environment of the square planar nickel(II) ions in $L1^{2-}$ compared to those in $L2^{2-}$ are revealed by an examination of the dihedral angles between the respective NiN_2 and NiS_2 planes: the longer alkyl chain in **1a** has caused some buckling and tetrahedral

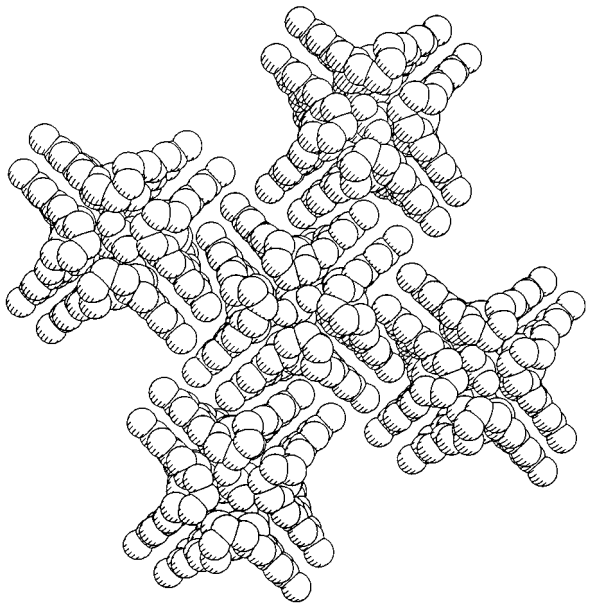

Figure 3. Space-filling diagram of part of a sheet of π−π-stacked $[Ni_2L1]^{2+}$ cations of **1a** [hydrogen atoms, anions, and solvent molecules omitted for clarity, with the exception of the central perchlorate ion, Cl(1)]

distortion away from square planar (15.4−18.9°), whereas an almost planar (slightly folded) arrangement is found in **2a** (2.3−6.1°).[16] A series of related mononickel acyclic complexes has been studied and a wide variation in properties was found depending on the degree of distortion.[30] To probe the significance of this distortion binding studies were undertaken and led to the formation and characterisation of **4**.

Red-black crystals of **4** · 2 MeCN suitable for X-ray crystal structure analysis were grown from the acetonitrile reaction solutions on standing. The structure determination (Figure 4, Tables 1 and 2) reveals that the thiocyanate anions are indeed coordinated to nickel(II). Interestingly both thiocyanate ions bind to one nickel atom, Ni(2), giving it a distorted octahedral geometry overall [Ni(2) is 0.010(2) Å out of the $N(macro)_2S_2$ plane] whilst the remaining nickel atom, Ni(1), remains square planar [Ni(1) is 0.036(2) Å out of the N_2S_2 plane]. Bond lengths to Ni(1) are in the usual range observed for square planar nickel(II) complexes and the corresponding bond lengths involving Ni(2) are ca. 0.2 Å longer as is typical of octahedral (high spin) nickel(II) complexes.[16,35,36]

Complex **4** is folded in the same way as complex **1a**: the two $N(macro)_2S_2$ planes intersect at 140.2(1)° and the two phenyl ring planes at 86.7(1)° in **4** compared to averages of 138.8(2)° and 85.3(4)°, respectively, for **1a**. Slightly larger S···S [2.79−2.83 in **1a** vs. 2.979(2) Å in **4**] and Ni···Ni separations [3.12−3.14 in **1a** vs. 3.2935(8) Å in **4**] are observed in **4**. The three-dimensional packing arrangements of **1a** and **4** are different as a result of the differences in anion template effects. Rather than the anion templating the packing together of the macrocyclic complexes, as is the case with the perchlorate ion in **1a**, the thiocyanate ions block the formation of all but one set of π−π interactions.

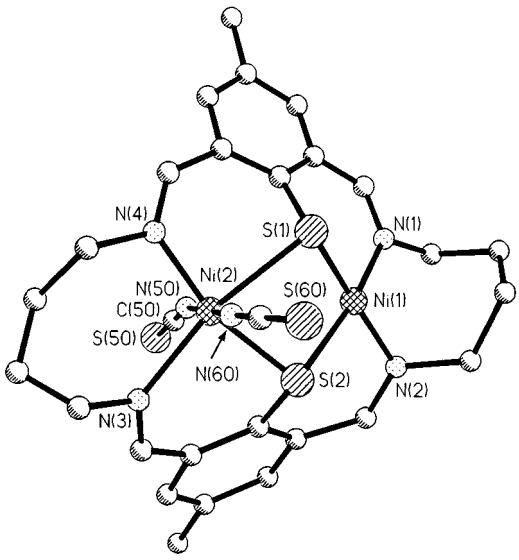

Figure 4. Perspective view of $[Ni_2L1(NCS)_2]$ **4** (hydrogen atoms and solvent molecules omitted for clarity)

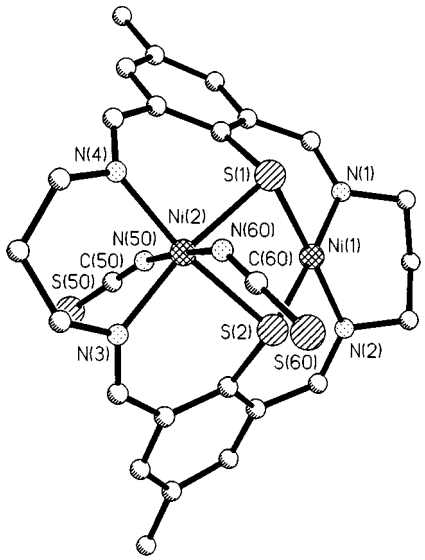

Figure 5. Perspective view of $[Ni_2L2(NCS)_2]$ **5** (hydrogen atoms and solvent molecule omitted for clarity)

The successful formation of **4** prompted us to test whether or not the analogous reaction could be carried out with the less tetrahedrally distorted, macrocyclic complex of the smaller ring $L2^{2-}$, $[Ni_2L2](ClO_4)_2$ **2b**. Red-black crystals of **5** · MeCN suitable for X-ray analysis were obtained, in low yield, from the reaction of **2b** with 2.2 equivalents of NaSCN in MeCN. A similar overall structure to that of **4** is revealed by the structure determination: one nickel atom remains square planar [Ni(1) is 0.003(1) Å out of the N_2S_2 plane] whilst the other is distorted octahedral [Ni(2) is 0.026(1) Å out of the $N(macro)_2S_2$ plane] and coordinated to both thiocyanate ions (Figure 5, Tables 1 and 2). The bond lengths to Ni(1) and Ni(2) are similar to those found in **4** and reflect the respective low spin and high spin configurations of these atoms. The smaller ring size of $L2^{2-}$ is still sufficient to accommodate the high-spin nickel(II) ion. However, there is sufficient ring strain induced by the change in spin state to promote Schiff-base hydrolysis (by traces of moisture) and ring opening, as the major product of the reaction with NaSCN is shown by IR spectroscopy to be a ring opened product (see above).

Comparison of the structure of the perchlorate derivative **2a** with the thiocyanate derivative **5** leads to similar trends to those obtained from the comparison of the corresponding $L1^{2-}$ analogues **1a** and **4**. Complex **5** is folded with the $N(macro)_2S_2$ planes intersecting at 142.21(6)° and the two phenyl ring planes, almost at right angles to one another, intersecting at 91.17(9)° [av. 146.4(2) and 102.4(4)° respectively in **2a**]. Slightly larger S···S [av. 2.839(5) in **2a** vs. 3.011(1) Å in **5**] and Ni···Ni separations [av. 3.146(2) in **2a** vs. 3.244(1) Å in **5**] are observed in **5**. Again the coordinated thiocyanate ions block all but one set of π-π interactions.

Complexes with adjacent square planar and octahedral nickel(II) ions have been reported previously.[14,18,35,37–39] Of these one of the most closely related examples is **A1**, a dinickel(II) complex derived from a "three-quarter" amine thiolate ligand (Figure 6).[39] In this complex both of the thiocyanate ions coordinated to the nickel ion which was bound to the secondary, as opposed to the primary, amine groups due to the slightly weaker field strength exerted by them. However, in complexes **4** and **5** the differing nickel(II) geometries have resulted despite the provision of potentially identical metal ion binding sites and this situation is much less common. We have observed this situation before for the macrocyclic thiolate complex **A2** (Figure 6), where the macrocycle provided potentially identical N(imine)N(amine)SO donor sites,[14][18] but the isolation of complexes **4** and **5** is an important extension of the series of dinickel thiolate complexes produced to date[11,14,16,18–21,25,39–43] as, until recently, it was thought that the $N(imine)_2S_2$ systems exclusively formed square planar complexes.

Table 1. Selected bond lengths (Å) in $[Ni_2L1](ClO_4)_2(MeCN)\cdot 1/4\,H_2O$ **1a**, $[Ni_2L1(NCS)_2]$ **4**, and $[Ni_2L2(NCS)_2]$ **5**

Bond lengths	**1a**	**4**	**5**
Ni(1)−N(1)	1.929(10)	1.944(3)	1.924(2)
Ni(1)−N(2)	1.928(10)	1.926(3)	1.935(2)
Ni(1)−S(1)	2.157(4)	2.1732(12)	2.2009(10)
Ni(1)−S(2)	2.152(3)	2.1987(12)	2.1836(10)
Ni(2)−N(3)	1.920(10)	2.073(3)	2.037(2)
Ni(2)−N(4)	1.939(9)	2.078(3)	2.024(2)
Ni(2)−S(1)	2.147(3)	2.3849(13)	2.3738(10)
Ni(2)−S(2)	2.167(3)	2.4080(12)	2.3608(11)
Ni(2)···O(11)	3.340(9)	−	−
Ni(2)−N(50)	−	2.071(4)	2.096(3)
Ni(2)−N(60)	−	2.065(4)	2.112(3)
Ni(1)···Ni(2)	3.115(2)	3.2935(8)	3.2437(11)
S(1)···S(2)	2.828(4)	2.979(2)	3.0112(12)

Table 2. Selected bond angles (°) in $[Ni_2L1](ClO_4)_2(MeCN)\cdot 1/4\ H_2O$ **1a**, $[Ni_2L1(NCS)_2]$ **4**, and $[Ni_2L2(NCS)_2]$ **5**

Bond angles	**1a**	**4**	**5**
N(1)−Ni(1)−N(2)	96.6(4)	94.97(14)	94.44(10)
N(1)−Ni(1)−S(2)	165.5(4)	167.23(11)	176.11(8)
N(1)−Ni(1)−S(1)	88.8(3)	94.28(10)	89.36(7)
S(2)−Ni(1)−N(2)	95.0(3)	86.80(11)	89.44(7)
S(2)−Ni(1)−S(1)	82.04(13)	85.90(4)	86.75(3)
N(2)−Ni(1)−S(1)	165.3(3)	167.88(11)	176.16(7)
N(3)−Ni(2)−N(4)	97.1(4)	106.46(13)	99.08(9)
N(3)−Ni(2)−S(2)	89.0(3)	87.71(9)	90.84(7)
N(4)−Ni(2)−S(2)	165.4(3)	165.51(10)	170.03(7)
N(3)−Ni(2)−S(1)	165.6(3)	164.30(9)	169.66(7)
N(4)−Ni(2)−S(1)	94.4(3)	89.12(10)	91.07(7)
S(2)−Ni(2)−S(1)	81.91(13)	76.85(4)	78.99(3)
N(60)−Ni(2)−N(50)	−	177.75(15)	175.80(9)
N(60)−Ni(2)−N(3)	−	90.81(13)	89.54(10)
N(50)−Ni(2)−N(3)	−	88.03(13)	86.30(9)
N(60)−Ni(2)−N(4)	−	88.58(13)	92.61(10)
N(50)−Ni(2)−N(4)	−	89.91(13)	88.54(9)
N(60)−Ni(2)−S(1)	−	91.51(11)	91.99(7)
N(50)−Ni(2)−S(1)	−	90.13(10)	92.02(7)
N(60)−Ni(2)−S(2)	−	88.15(10)	88.48(7)
N(50)−Ni(2)−S(2)	−	93.73(10)	91.08(7)
Ni(1)−S(1)−Ni(2)	92.73(13)	92.41(4)	90.23(4)
C(1)−S(1)−Ni(1)	97.7(4)	109.32(14)	102.77(10)
C(1)−S(1)−Ni(2)	107.3(4)	102.39(15)	98.68(10)
C(14/13)−S(2)−Ni(1)	105.7(4)	98.25(14)	104.23(10)
C(14/13)−S(2)−Ni(2)	97.4(4)	100.40(14)	101.20(10)
Ni(1)−S(2)−Ni(2)	92.32(13)	91.16(4)	91.00(3)

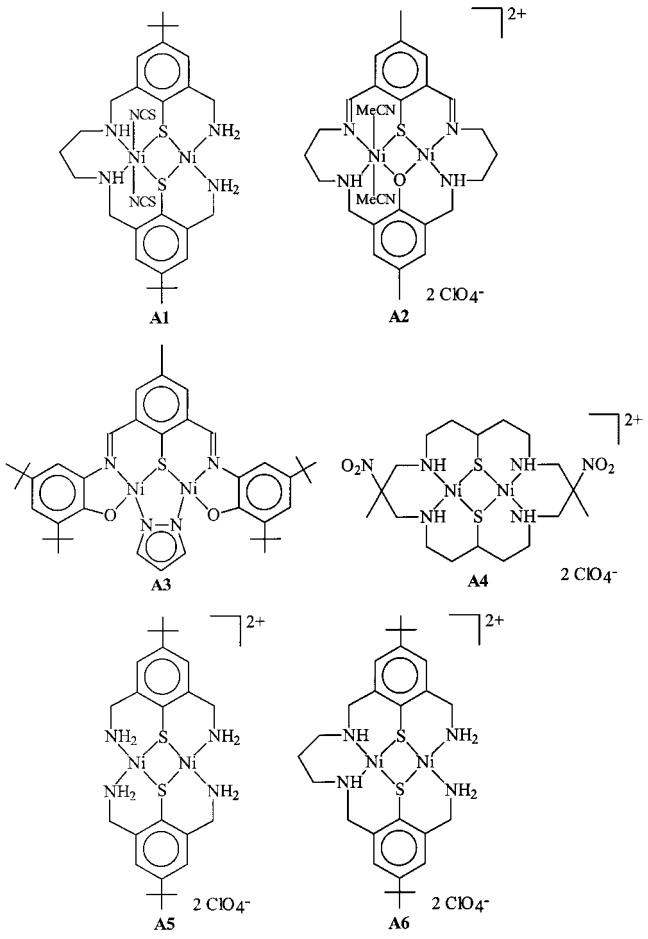

Figure 6. Dinickel(II) thiolate complexes **A1**−**A6**

NMR Studies

In the non-coordinating solvent $[D_3]MeNO_2$ **1**−**3** all gave easily assigned diamagnetic ^1H- and ^{13}C-NMR spectra. In coordinating solvents such as $[D_3]MeCN$ and $[D_7]DMF$ complexes **1**−**3** have some tendency to coordinate solvent molecules in the otherwise vacant axial sites leading to traces of paramagnetic species in solution. The ^1H-NMR spectrum obtained at elevated temperatures for **2** in $[D_3]MeCN$ could be assigned but that obtained for **1** was too broad over the temperature range studied (253 to 333 K). In contrast, **3**, the amine analogue of **2**, gave a reasonably sharp ^1H-NMR spectrum at ambient temperature showing that this complex remains close to diamagnetic even in acetonitrile solution. The amine proton signal for complex **3** has now been correctly identified[19] via a NH/ND exchange experiment: a few drops of a $[D_3]MeOD/D_2O$ (95:5) mixture was added to a solution of **3** in $[D_3]MeNO_2$ which caused the signal at 3.58 ppm to disappear over a period of days. In $[D_7]DMF$ no ^1H-NMR spectrum was obtained for complexes **1** and **2** whilst complex **3** gave a very broad spectrum. Consistent with this, an axial interaction with a DMF molecule was observed in the crystal structure of the hexafluorophosphate salt of **2**.[20]

The NMR data, in both $[D_3]MeNO_2$ (**1**−**3**) and $[D_3]MeCN$ (**2**, **3**), indicate that the macrocycles remain intact in these solvents.

Cyclic Voltammetry Studies

Of particular interest in this series of compounds are the effects of (a) increasing the size of the macrocyclic cavity, $L1^{2-}$ vs. $L2^{2-}$, (b) changing the nature of the nitrogen donors, from imine groups in **2** to amine groups in **3**,[19] and (c) changing from thiophenolate donors in **2** to phenolate donors in **6**. Representative cyclic voltammograms for compounds **1**−**3** and **6** in MeCN are presented in Figure 7 and the potentials of the four well-separated (> 0.2 V) one-electron redox processes for **1**−**3** are provided in Table 3. The three well-separated (> 0.2 V) one-electron redox processes for **6** occur at -1.40^{I}, $+1.05^{QR}$, and $+1.26^{I}$ V (referenced to 0.01 M $AgNO_3/Ag$ and recorded at 200 mV s^{-1}). The redox processes are considered to be predominantly metal centred (vide infra) and the following discussion is made in light of this assignment.

Intriguingly the $[Ni_2Lj]^{2+/3+}$ and $[Ni_2Lj]^{3+/4+}$ potentials ($j = 1-3$) show relatively small shifts upon quite large changes in the ligation of the nickel centres. The peak separation, ΔE, for the first process in all three systems was comparable to that of ferrocene indicating that this is a reversible process in each case, a conclusion that is further supported by analysis of the ratio of peak currents and scan rate dependence.[44] Like the $[Ni_2Lj]^{2+/3+}$ process the position of the $[Ni_2Lj]^{3+/4+}$ process shifts very little from $j = 1$ to $j = 3$. However in each case the peak separation for this second process is larger than that observed for the first process, and the ratio of the peak currents differs significantly from unity, indicating that the $[Ni_2Lj]^{3+/4+}$ couple is a

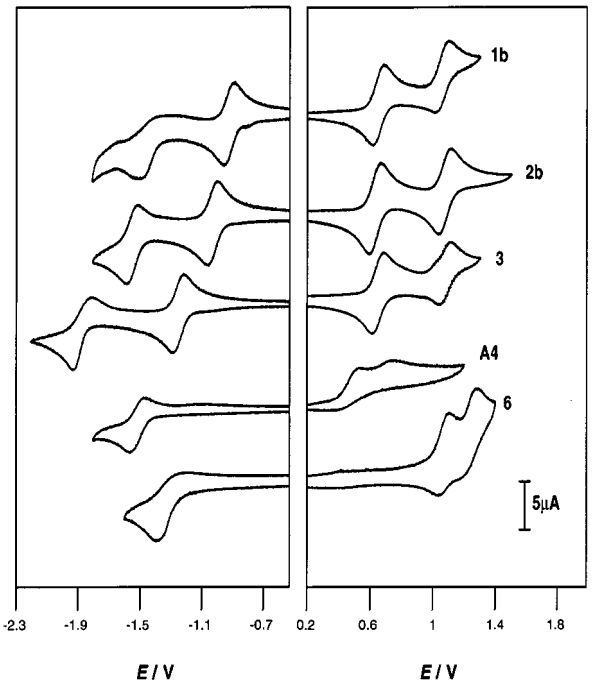

Figure 7. Cyclic voltammograms of complexes (listed from top to bottom) **1b**, **2b**, **3**, **A4**, and **6** in MeCN (200 mV s^{-1}, 0.1 M NEt_4ClO_4, platinum electrode, vs. 0.01M $AgNO_3$/Ag)

Table 3. Potentials ($E_{1/2}$, V) and E (V) for the dinickel complexes $[Ni_2Lj]^{2+}$, (j = 1−3,′). All data were referenced to 0.01 M $AgNO_3$/Ag and recorded at 200 mV s^{-1}. In all cases the Fc/Fc^+ couple, added as an internal reference, occurred at +0.13 V with ΔE = 0.07 V

Complex	$[Ni_2Lj]^{0/+}$	$[Ni_2Lj]^{+/2+}$	$[Ni_2Lj]^{2+/3+}$	$[Ni_2Lj]^{3+/4+}$
1b[a]	−1.45 (0.16)^{I}	−0.92 (0.07)^{R}	+0.64 (0.06)^{R}	+1.05 (0.08)^{QR}
2b[a]	−1.46 (0.07)^{R}	−1.01 (0.06)^{R}	+0.63 (0.08)^{R}	+1.07 (0.08)^{QR}
3[a]	−1.86 (0.10)^{QR}	−1.18 (0.08)^{R}	+0.69 (0.08)^{R}	+1.10 (0.08)^{QR}
1b[b]	−1.49 (0.09)^{QR}	−0.95 (0.09)^{R}	+0.50^{I}	–
2b[b]	−1.49 (0.07)^{R}	−1.03 (0.07)^{R}	+0.40 (0.08)^{R}	+0.82 (0.10)^{I}
3[b]	−1.86 (0.09)^{QR}	−1.21 (0.08)^{QR}	+0.41 (0.11)^{QR}	+0.61^{I}
2b[c]	−1.42^{I}	−1.10^{I}	–	–
6[a]	–	−1.40^{I}	+1.05 (0.10)^{QR}	+1.26^{I}

[a] Solvent = MeCN, [b] solvent = DMF, [c] solvent = $MeNO_2$. ^{R} reversible, ^{QR} quasireversible, ^{I} irreversible (hence in this case E_{pc} or E_{pa} is quoted not $E_{1/2}$); these assignments were made on the basis of peak separation ΔE (cf. ferrocene), analysis of the ratio of peak currents and scan rate dependence of $E_{1/2}$.[44] Electron counts (in MeCN): **1b** $[Ni_2L1]^{2+} \rightarrow [Ni_2L1]^{+}$ 0.87 e-equivalent; **2b** $[Ni_2L2]^{2+} \rightarrow [Ni_2L2]^{3+}$ 0.95 e-equivalent and $[Ni_2L2]^{3+} \rightarrow [Ni_2L2]^{4+}$ 0.88 e-equivalent; **3** $[Ni_2L3]^{2+} \rightarrow [Ni_2L3]^{3+}$ 0.98 e-equivalent.

quasi-reversible process in all three cases.[44] Thiolate donors are known to stabilise high metal ion oxidation states[45] so the fact that the two one-electron oxidation processes observed for the phenolate analogue, complex **6**, occur at much more positive potentials is consistent with expectations.[46−48] Changes to the ligand, either by increasing the macrocyclic cavity size or by changing from imines to amines, usually has a much larger effect on the potentials than is the case here.[49][50]

In contrast, the peak positions for the $[Ni_2Lj]^{2+/+}$ and $[Ni_2Lj]^{+/0}$ processes (j = 1−3) are very sensitive to the changes in the macrocyclic ligand. The $[Ni_2Lj]^{2+/+}$ processes are reversible for all three complexes **1**−**3**. The $[Ni_2Lj]^{2+/+}$ process occurs at −1.01 V for $[Ni_2L2]^{2+}$ while the complex with the larger macrocyclic cavity, $[Ni_2L1]^{2+}$, is easier to reduce, by 90 mV, and the complex of the tetra-amine macrocycle, $[Ni_2L3]^{2+}$, is harder to reduce, by 170 mV. Only a single one-electron irreversible reduction process is observed for the phenolate analogue, complex **6**, and it occurs at a significantly more negative potential, as is expected[45] (although not *always* observed)[11] due to the presence of the harder phenolate donors. In only one of the three systems was the $[Ni_2Lj]^{+/0}$ process truly reversible, namely the $[Ni_2L2]^{+/0}$ couple. The $[Ni_2L1]^{+/0}$ process is irreversible whilst the $[Ni_2L3]^{+/0}$ process is quasi-reversible. These $[Ni_2Lj]^{+/0}$ processes shift in the same direction as the shifts observed for the $[Ni_2Lj]^{2+/+}$ processes. The $[Ni_2L2]^{+/0}$ and $[Ni_2L1]^{+/0}$ processes occur at a similar potentials (−1.46 and −1.45 V, respectively) whereas the $[Ni_2L3]^{+/0}$ process is 370 mV more negative {ie. $[Ni_2L3]^{+}$ is harder to reduce}. No second reduction process was observed for **6**.

Overall the $[Ni_2Lj]^{2+/+}$ and $[Ni_2Lj]^{+/0}$ potentials for the complexes of the tetra-imine-containing ligands $L1^{2-}$ and $L2^{2-}$, **1** and **2**, are significantly less negative than those for the complex of the tetra-amine-containing ligand $L3^{2-}$, **3**. The imine-containing ligands stabilise the reduced metal centre(s) more effectively than the amine-containing ligand (which has no imine π* orbital).[49][50] It had been hoped that conversion of the hydrolytically unstable imine bonds to relatively stable amine bonds would make the reductive electrochemistry more reversible as decomposition via, for instance, water attack of the adjacent imine bond would no longer be possible. However these redox processes are actually less reversible than those of the tetra-imine analogue **2**.

A study of a large number of mono nickel(II) tetra-aza macrocycles has shown that there is a correlation between the size of the macrocycle cavity and the potentials, with the larger cavities stabilising the nickel(I) oxidation state.[49] This has been interpreted as indicating that the d^9 nickel(I) ion is larger than the d^8 nickel(II) ion and is therefore better accommodated by a larger ring, resulting in a less negative potential for the $Ni^{2+/+}$ process.[49][51] Our results are consistent with this correlation.

As the NMR studies (above) indicated that some solvent coordination is occurring in MeCN and DMF solutions but not in $MeNO_2$, cyclic voltammograms were also run in DMF and $MeNO_2$. The results for **2** are shown in Figure 8 and Table 3. In DMF and MeCN, the $[Ni_2L2]^{2+/+}$ and $[Ni_2L2]^{+/0}$ processes are relatively insensitive to the change in solvent indicating that the formally $Ni^{II}Ni^{I}$ and Ni^{I}_2 species coordinate solvent molecules only weakly, if at all. However, in DMF, the $[Ni_2L2]^{3+/4+}$ process is a substantial 230 mV less positive {$[Ni_2L2]^{3+}$ is easier to oxidise in DMF than in MeCN}. This shift is to be expected as the Ni^{III} ion will be stabilised by axial coordination of solvent molecules,[11][51] and DMF has a greater tendency to bind axially than MeCN.[48] The results obtained in the non-coordi-

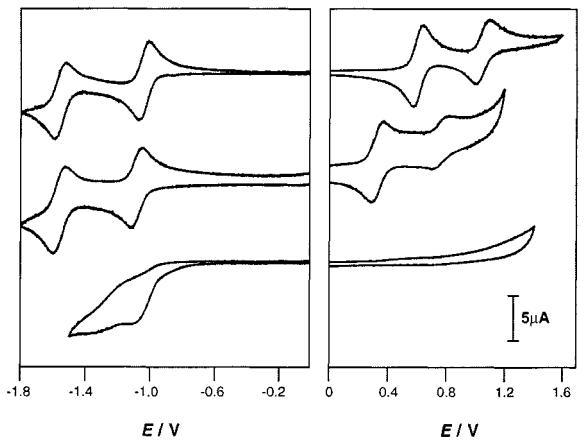

Figure 8. Solvent dependence of cyclic voltammograms of **2b**: comparison of cyclic voltammograms obtained in MeCN (top), DMF (middle), and $MeNO_2$ (bottom) (200 mV s^{-1}, 0.1 M NEt_4ClO_4, platinum electrode, vs. 0.01M $AgNO_3$/Ag)

nating solvent, $MeNO_2$ (Figure 8, Table 3), are consistent with this explanation. No oxidation processes are observed for **2** within the $MeNO_2$ solvent window: two reduction processes are observed but they are irreversible so a meaningful comparison of the potentials is not possible. These observations are consistent with the processes being largely metal centred.

The results of this solvent dependence study are also consistent with those obtained for an acyclic dinickel thiophenolate complex **A3** (Figure 6):[11] the reduction processes varied only slightly with solvent (CH_2Cl_2, acetone, THF, PrCN, and DMF) indicating that there was little or no solvent coordination to the nickel(I) centres whereas the first oxidation process was less positive in DMF than in the other solvents investigated [ie. CH_2Cl_2 (where the processes became reversible), acetone, and THF], which was attributed to solvent coordination to the nickel(III) centres.

As expected, the cyclic voltammetry results for complex **2b** in MeCN are consistent within experimental error with those reported for the perchlorate salt **2a**[16,52] and for the hexafluorophosphate salt of **2**.[22] To date no electrochemical properties have been reported for the other Schiff base macrocyclic di- and tetra-nickel(II) complexes derived from the 2,6-diformylthiophenolate head unit.[23][24] The cyclic voltammogram we obtained in MeCN for the dark orange dinickel(II) aliphatic-thiolate macrocyclic complex **A4** (Figure 6) is shown for comparison in Figure 7.[25] The relatively electron-rich aliphatic-thiolate donors stabilise Ni^{III} and destabilise Ni^{I} relative to the aromatic-thiolate donors in Lj^{2-}, $j = 1-3$. Changing the ligation around the nickel(II) ions from two separate tridentate ligands, complex **A5**, to one "three-quarter" hexadentate ligand, complex **A6** (Figure 6), results in improved reversibility of the two one-electron, metal centred, reductions in DMF.[39] As expected, on completely encircling the nickel ions with a hexadentate *macrocyclic* ligand, as in complexes **1–3**, the reversibility improves still further.

In summary, in these three macrocyclic dinickel(II) thiolate systems, $[Ni_2Lj]^{2+}$ where $j = 1-3$, the two one-electron oxidation processes are relatively insensitive to the changes made to the ligand but are sensitive to changes in solvent (MeCN vs. DMF vs. $MeNO_2$). As we believe the oxidation processes, $[Ni_2Lj]^{2+/3+}$ and $[Ni_2Lj]^{3+/4+}$, are primarily metal centered (vide infra) it seems likely that the relatively invariant value of the potentials for $j = 1-3$ for a particular solvent is largely due to the consistent supply of an axial donor (either N of MeCN or O of DMF). In contrast the $[Ni_2Lj]^{2+/+}$ and $[Ni_2Lj]^{+/0}$ processes, which are also believed to be primarily metal centred, are significantly influenced by changes to the ligand but are relatively insensitive to changes in solvent (MeCN vs. DMF). As expected, a change in the nitrogen donors from imines to amines made the potentials more negative, while increasing the size of the macrocyclic cavity made the potentials slightly less negative. The formally nickel(I) centres are expected to be square planar hence the lack of solvent dependence.

EPR Spectra

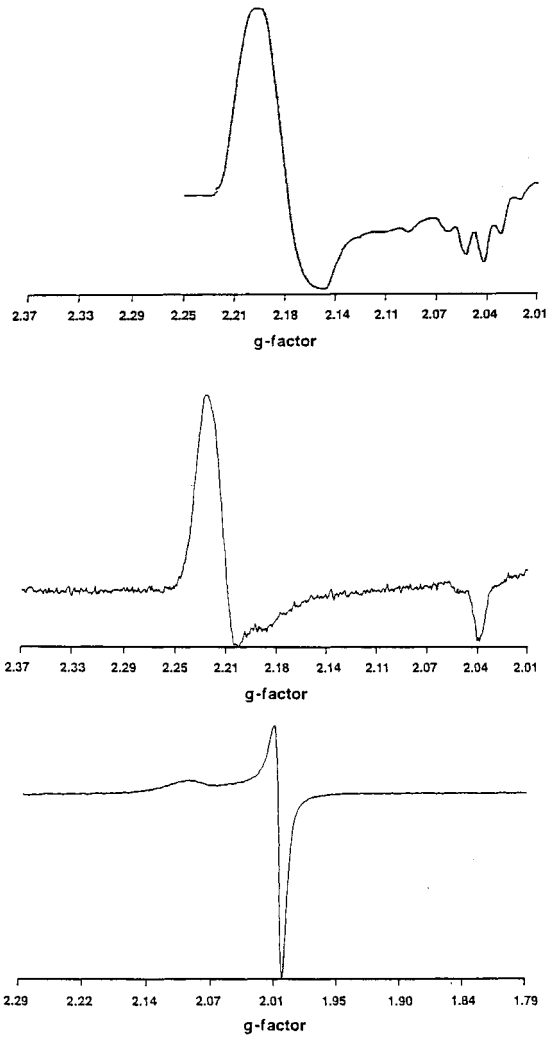

Figure 9. EPR spectra of 10^{-4} mol L^{-1} chemically generated $[Ni_2L2]^{3+}$ (top, 10 mW, 9.142 GHz), electrochemically generated $[Ni_2L2]^{3+}$ (middle, 0.816 mW, 9.284 GHz), and $[Ni_2L3]^{+}$ (bottom, 0.766 mW, 9.284 GHz), in MeCN at 77 K

Due to the instability of the majority of the redox products on a time scale of minutes (cf. the cyclic voltammetry time scale) EPR spectroscopic studies were limited to the oxidation products (both electrochemically and chemically generated) of complexes **2** and **3**, and the reduction products (electrochemically generated) of complexes **1** and **3**.

The EPR spectrum of the purple solution obtained by one electron electrochemical oxidation of **2b** at 1.0 V vs Ag wire is shown in Figure 9. The spectrum is characteristic of the presence of an axial Ni^{III} centre, with $g_{||} = 2.04$ and $g_{\perp} = 2.22$, indicating the presence of a mixed valent Ni^{II}-Ni^{III} centre.[51] Similar EPR behaviour was observed for the purple, electrochemically generated $[Ni_2L3]^{3+}$ species.

Chemical oxidation of an MeCN solution of **2a** with aqueous Co^{III} in 1 M $HClO_4$ yielded a purple solution which again gave an EPR spectrum typical of an axial Ni^{III} centre, with $g_{||} = 2.04$ and $g_{\perp} = 2.17$. The $g_{||}$ feature shows hyperfine splitting associated with two axially coordinated MeCN solvent molecules.

The reduction products of complex **2** were not stable enough to be studied by EPR, however, those of complexes **1** and **3** were investigated (Figure 9). The orange-brown one-electron reduction products of **1** and **3** showed very similar EPR behaviour consistent with a metal-centred reduction to a d^9 Ni^{I} centre ($g_{||} = 2.11$, $g_{\perp} = 2.00$).[51]

These results are consistent with both the first one-electron oxidations and reductions being largely metal based with little delocalisation onto the ligand. Importantly there is no evidence for the presence of organic radicals. The nature of the formally Ni^{I}_2 and Ni^{III}_2 species could not be established due to the low stability of these products.

Electronic Spectra

In $MeNO_2$, MeCN, and DMF the red dinickel(II) complexes **1**−**3** all have an absorption band in the range 490−520 nm (ε = 900−1800 L mol^{-1} cm^{-1}) which is assigned as a ligand-to-metal charge transfer (LMCT) transition, $S\pi \rightarrow Ni$.[5][39] This band occurs at slightly higher energy in the case of the amine complex **3** (490 nm) than in the imine analogue **2** (510 nm) leading to the former being somewhat more red in colour than the latter. In DMF, in addition to the 490−520 nm band, some further low intensity bands/shoulders are observed at longer wavelengths which are presumably due to axial solvent coordination to least one of the two nickel atoms.[39] Only in the case of complexes **1** and **3** can distinct bands be clearly identified: the lowest energy band, $^3A_{2g} \rightarrow {}^3T_{2g}$, occurs at 990 nm (80 L mol^{-1} cm^{-1}) for **3** and at 860 nm (25 L mol^{-1} cm^{-1}) for **1**. This corresponds to a smaller Δ_O for **3** (10,101 cm^{-1}) than for **1** (11,630 cm^{-1}), consistent with the NMR finding that **3** is less able to bind solvent molecules axially than **1**. In all cases further bands are observed at higher energy, below 380 nm, due to intraligand transitions. Over a period of weeks both the $MeNO_2$ and DMF solutions of **1**−**3** slowly decolorise whereas the acetonitrile solutions remain red.

The instability of the majority of the redox products on a time scale of minutes limited the UV/Vis studies to the oxidation products (both electrochemically and chemically generated) of complex **2** and the one-electron reduction product (electrochemically generated) of complex **1**.

Complex **1b** was electrochemically reduced in MeCN at −1.10 V vs. 0.01 M $AgNO_3$/Ag (87% of one-electron equivalent) resulting in an orange solution: the 510 nm band diminishes in absorbance and an isobestic point is observed at 495 nm (Figure 10). This mixed valent complex, $[Ni_2L1]^+$, is reasonably stable at ambient temperature under argon but attempts to further reduce it by one electron were unsuccessful.

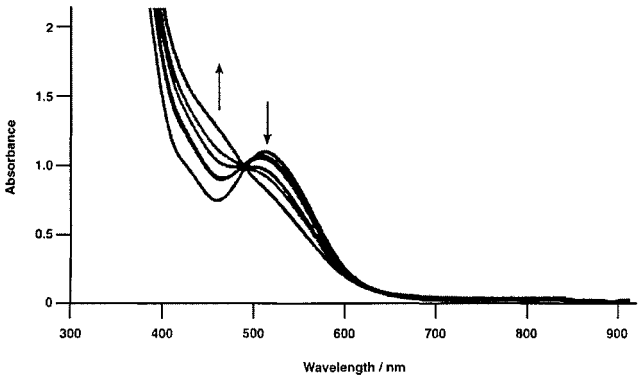

Figure 10. Electrochemical one electron reduction of **1b** in MeCN followed by UV/Vis spectroscopy

Controlled potential electrolysis of **2b** in MeCN at +0.90 V vs. 0.01 M $AgNO_3$/Ag removes one-electron (97%) giving a purplish-coloured solution: a new band develops at approximately 870 nm (isobestic point at ca. 390 nm). This mixed valent complex, $[Ni_2L2]^{3+}$, is reasonably stable at ambient temperature under argon. When a second electron is removed from this sample, by holding the potential at +1.40 V vs. 0.01 M $AgNO_3$/Ag, a dark green solution results, and the 870 nm band bleaches out. Nickel(III) complexes are typically green in colour.[53] Removal of the second electron to form $[Ni_2L2]^{4+}$ is nontrivial due to the low stability of this fully oxidised species.

Complex **2a** was also chemically oxidised by titrating with CAN [ammonium cerium(IV) nitrate]. The titration with the first equivalent of CAN (Figure 11) resulted in a new absorption band at 870 nm. When the titration was continued with the second equivalent of CAN (Figure 11) a dark green solution resulted. During this second stage of the titration the feature at 870 nm decreased in absorbance, as did all of the other bands. Due to the instability of this fully oxidised species it is not possible to determine whether the 870 nm band (11,494 cm^{-1}, ε = 1,320 L mol cm^{-1}) observed for the mixed valent $[Ni_2L1]^{3+}$ complex is due to a ligand to nickel(III) charge transfer transition or to a Class II intervalence charge transfer transition (the bandwidth at half height is approximately 5400 cm^{-1} which is greater than the calculated value of 5153 cm^{-1}).[54]

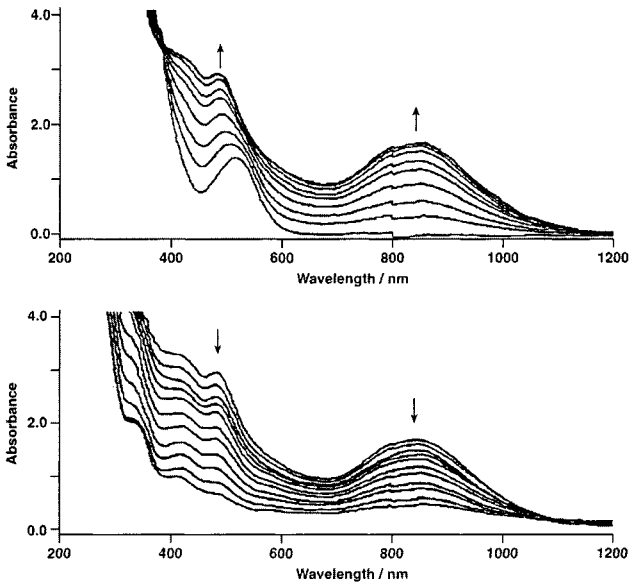

Figure 11. Titration of a 2.7 mL aliquot of a 6.34×10^{-4} mol L^{-1} MeCN solution of **2a**, firstly with one (top) and then with a second (bottom) equivalent of CAN (0.0785 mol L^{-1}, aliquots of 2 μL per scan)

Conclusion

The nickel coordination chemistry of $L1^{2-}$ and $L2^{2-}$ has produced a range of attractive and interesting products, including rare examples of adjacent N_2S_2 and N_4S_2 nickel(II) ions despite the provision of potentially equivalent binding sites. The aim of increasing the degree of tetrahedral distortion over that found in the macrocycle $L2^{2-}$ by increasing the macrocycle cavity size, despite the strong preference of the nickel ions to be square planar in this donor environment, has been achieved with $L1^{2-}$. This increased tetrahedral distortion confers a greater tendency for dinickel(II) complexes of $L1^{2-}$ to bind molecules axially. The ability to manipulate and control the environments of the nickel(II) ions in this way is important with respect to developing model complexes suitable for binding/reactivity studies, and is facilitated by the wide range of geometries which the bridging thiolate donors can adopt.

Experimental Section

Measurements were carried out as previously described,[16] with the exception of most of the NMR spectra which, where noted, were obtained on a Varian 500 MHz spectrometer. Magnetic moments were obtained on a Johnson Matthey Alfa Products Mk1 magnetic susceptibility balance. Electrochemical experiments were performed using a PAR 273A potentiostat/galvinostat in a 3-electrode cell (design by Dr. E. Bothe and Prof. K. Wieghardt, MPI für Strahlenchemie) using Pt working and counter electrodes and a $Ag/AgNO_3$ reference electrode. *tert*-Butyl ammonium perchlorate (recrystallised twice from H_2O and dried in vacuo at room temperature) was used as the supporting electrolyte. All solutions were degassed thoroughly with argon and an argon atmosphere was maintained during the experiments. (*S*)-(2,6-Diformyl-4-methylphenyl)dimethylthiocarbamate[16] and $[Ni_2L'Cl_2]$[27] were prepared according to the literature procedures. Isopropanol (IPA) was stored over CaO, then decanted and distilled. HPLC grade MeCN and DMF were distilled from CaH_2 (DMF in vacuo) immediately before use. Reactions were carried out using Schlenk techniques.

CAUTION: *Perchlorate salts are potentially explosive and should therefore be handled with appropriate care.*

$[Ni_2L1](ClO_4)_2 \cdot MeCN \cdot 1/4\ H_2O$ (1a): (*S*)-(2,6-Diformyl-4-methylphenyl)dimethylthiocarbamate (0.251 g, 1.00 mmol) in IPA (80 cm^3) was brought to reflux. NaOH (0.040 g, 1.00 mmol) was added, the resulting orange solution refluxed for 5 hours, then $Ni(ClO_4)_2 \cdot 6\ H_2O$ (0.365 g, 1.00 mmol) in IPA (20 cm^3) and 1,4-diaminobutane (0.088 g, 1.00 mmol) in IPA (20 cm^3) were added. After 4 hours the mixture was filtered hot to obtain **1a** as an impure red-brown solid. Repeated fractional recrystallisation from MeCN by vapour diffusion of diethyl ether gave $[Ni_2L1](ClO_4)_2(MeCN) \cdot 1/4\ H_2O$ **1a** as large red crystals suitable for X-ray structural analysis. The sample was washed with H_2O to give analytically pure **1a** (0.170 g, 42%). (Found: C 40.6, H 4.2, N 9.0, S 8.0, Cl 8.6. $C_{28}H_{33.5}Cl_2N_5Ni_2O_{8.25}S_2$ requires C 40.8, H 4.1, N 8.5, S 7.8, Cl 8.6%); λ_{max}/nm (MeCN) (ε/L mol^{-1} cm^{-1}) 510 (1 800); $\tilde{\nu}/cm^{-1}$ (KBr disk, inter alia) 1624, 1090, 623; Λ_m(MeCN) = 268 mol^{-1} cm^2 Ω^{-1} (c.f. 220−300 mol^{-1} cm^2 Ω^{-1} for a 2:1 electrolyte in MeCN);[55] FAB mass spectrum *m*/*z* 578 $[Ni_2L1]^+$.

$[Ni_2L1](CF_3SO_3)_2 \cdot H_2O$ (1b): The reaction was performed as for $[Ni_2L1](ClO_4)_2$ but nickel(II) trifluoromethansulfonate hexahydrate (0.465 g, 1.00 mmol) was used instead of nickel(II) perchlorate hexahydrate. In contrast to $[Ni_2L1](ClO_4)_2$ the reaction solution became clear red-brown on addition of the amine and after two hours at reflux the solution was reduced in volume in vacuo to ca. 30 cm^3. From this solution red single crystals of $[Ni_2L1](CF_3SO_3)_2 \cdot H_2O$ were grown by vapour diffusion of diethyl ether (0.171 g, 38%). (Found C 37.7, H 4.0, N 6.1, S 13.9. $C_{28}H_{32}F_6N_4Ni_2O_7S_4$ requires C 37.5, H 3.6, N 6.3, S 14.3%); $\tilde{\nu}/cm^{-1}$ (KBr disk, inter alia) 3526, 3462, 1623, 1614, 1257, 1026, 636; δ_H (500 MHz, CD_3NO_2, 298 K): 8.03 (4 H, s), 7.60 (4 H, s), 3.97, 3.65 (4 H, t; 4 H, d), 2.39 (6 H, s), 3.45, 2.25 (4 H, d; 4 H,q) δ_C (125 MHz, CD_3NO_2, 298 K): 169.4, 141.8, 140.5, 136.2, 121.7, 61.7, 27.5, 20.9; λ_{max}/nm (MeCN) (ε/L mol^{-1} cm^{-1}) 510 (1800), ($MeNO_2$) 515 (1410), (DMF) 520 (900), 860 (25); Λ_m(MeCN) = 280 mol^{-1} cm^2 Ω^{-1} (c.f. 220−300 mol^{-1} cm^2 Ω^{-1} for a 2:1 electrolyte in MeCN);[55] FAB mass spectrum *m*/*z* 578 $[Ni_2L1]^+$; μ = 0.0 BM.

$[Ni_2L2](ClO_4)_2$ (2a): A slight modification of the synthesis reported previously:[16] (*S*)-(2,6-Diformyl-4-methylphenyl)dimethylthiocarbamate (0.251 g, 1.00 mmol) in IPA (80 cm^3) was brought to reflux. NaOH (0.040 g, 1.00 mmol) was added, the resulting orange solution refluxed for 5 hours. Nickel(II) perchlorate hexahydrate (0.365 g, 1.00 mmol) in IPA (20 cm^3) was then added. To the dark red-brown mixture was added 1,3-diaminopropane (0.074 g, 1.00 mmol) in IPA (20 cm^3). The mixture was refluxed for five hours and then filtered whilst hot. The resulting red-brown solid was repeatedly recrystallised from MeCN by vapour diffusion of diethyl ether to remove the brown impurity yielding $[Ni_2L2](ClO_4)_2$ as large red single crystals (0.161 g, 43%). (Found: C 38.4, H 3.7, N 7.4, S 8.0, Cl 9.8. $C_{24}H_{26}Cl_2N_4Ni_2O_8S_2$ requires C 38.4, H 3.5, N 7.5, S 8.5, Cl 9.4%); $\tilde{\nu}/cm^{-1}$ (KBr disk, inter alia) 1615, 1084, 622; δ_H (300 MHz, CD_3CN, 343 K) reference external TMS: 9.48 (4 H, s), 7.54 (4 H, s), (ca. 4.50, ca 4.31) (4 H, t, br; 4 H, t, br), 2.46 (6 H, s), (2.24, 1.64) (2 H, d; 2 H, s). λ_{max}/nm (MeCN) (ε/L mol^{-1} cm^{-1}) 510 (1600), Λ_m(MeCN) = 265 mol^{-1} cm^2 Ω^{-1} (c.f. 220−300 mol^{-1} cm^2 Ω^{-1} for a 2:1 electrolyte in MeCN);[55] FAB mass spectrum *m*/*z* 550 $[Ni_2L2]^+$.

$[Ni_2L2](CF_3SO_3)_2$ (2b): The reaction was performed as for $[Ni_2L2](ClO_4)_2$ but nickel(II) trifluoromethansulfonate hexahydrate (0.465 g, 1.00 mmol) was used instead of nickel(II) perchlorate hexahydrate. In contrast to $[Ni_2L2](ClO_4)_2$ the reaction solution became clear red-brown on addition of the amine. After two hours at reflux the solution was reduced in volume in vacuo to ca. 5 cm^3, 10 cm^3 of MeCN added and red crystals of $[Ni_2L2](CF_3SO_3)_2$ obtained by vapour diffusion of diethyl ether (0.14 g, 33%). (Found: C 36.4, H 3.5, N 6.3, S 14.8. $C_{26}H_{26}F_6N_4Ni_2O_6S_4$ requires C 36.7, H 3.1, N 6.6, S 15.1%); $\tilde{\nu}/cm^{-1}$ (KBr disk, inter alia) 1615, 1259, 1026, 637; δ_H (500 MHz, CD_3NO_2, 298 K): 7.93 (4 H, s), 7.56 (4 H, s), 4.38, 3.80 (4 H, t,; 4 H, d), 2.37 (6 H, s), 2.30, 1.60 (2 H, d; 2 H,q) δ_C (125 MHz, CD_3NO_2, 298 K): 167.9, 141.6, 140.1, 135.9, 123.0, 63.1, 29.3, 20.8. λ_{max}/nm (MeCN) (ε/L mol^{-1} cm^{-1}) 510 (1500), ($MeNO_2$) 510 (1480), (DMF) 510 (1040); Λ_m(MeCN) = 265 mol^{-1} cm^2 Ω^{-1} (c.f. 220−300 mol^{-1} cm^2 Ω^{-1} for a 2:1 electrolyte in MeCN);[55] FAB mass spectrum *m*/*z* 550 $[Ni_2L2]^+$; μ = 0.0 BM.

$[Ni_2L3](ClO_4)_2$ (3): To an ice-cold, fine particulate suspension of $[Ni_2L2](CF_3SO_3)_2$ **2b** (0.13 g, 0.18 mmol) in methanol (40 cm^3), was added $NaBH_4$ (0.030 g, 0.77 mmol) in water (2 cm^3). The reaction mixture was allowed to warm to room temperature, stirred for one hour and then refluxed for a further two hours. Then 5% $HClO_{4(aq)}$ (20 cm^3) was added and the mixture refluxed for one hour before being filtered whilst hot to remove $[Ni_2L3](ClO_4)_2$ as a red powder. Further crops were obtained by slow evaporation of the reaction filtrate (0.106 g, 80%). (Found C 37.5, H 4.8, N 7.2, S 8.7, Cl 9.3. $C_{24}H_{34}Cl_2N_4Ni_2O_8S_2$ (**3**) requires C 38.0, H 4.5, N 7.4, S 8.5, Cl 9.3%); $\tilde{\nu}/cm^{-1}$ (KBr disk, inter alia) 3220, 1603, 1096, 622; δ_H (500 MHz, CD_3NO_2, 298 K) 7.20 (4 H, s), 3.68 (4 H, d), 3.59 (4 H, d), 3.58 (4 H, s), 2.92 (4 H, td), 2.51 (4 H, dt), 2.25 (6 H, s), 2.02 (2 H, m), 1.85 (2 H, m); δ_C (125 MHz, CD_3NO_2, 298 K) 140.3, 135.6, 134.2, 121.7, 56.2, 50.4, 27.1, 21.1; λ_{max}/nm (MeCN) (ε/L mol^{-1} cm^{-1}) 490 (1500), ($MeNO_2$) 490 (1430), (DMF) 490 (900), 990 (80); Λ_m(MeCN) = 280 mol^{-1} cm^2 Ω^{-1} (c.f. 220−300 mol^{-1} cm^2 Ω^{-1} for a 2:1 electrolyte in MeCN);[55] FAB mass spectrum *m*/*z* 558 $[Ni_2L3]^+$; μ = 0.0 BM.

$[Ni_2L1(NCS)_2]$ (4): Complex **1b** (0.040 g, 0.046 mmol) was dissolved in MeCN (2 cm^3) to give a deep red solution. To this was added, in a dropwise fashion, a colorless solution of sodium thiocyanate (0.0085 g, 0.103 mmol) in MeCN (3 cm^3). Over time the solution became colorless and red-black crystals of **4** developed. These were filtered off and dried under vacuum (0.027 g, 83%). (Found: C 48.2, H 4.5, N 12.4, S 18.1. $C_{28}H_{30}N_6Ni_2S_4$ (**4**) requires C 48.3, H 4.3, N 12.1, S 18.4%); $\tilde{\nu}/cm^{-1}$ (KBr disk, inter alia) 2081, 1628; λ_{max}/nm (MeCN) (ε/L mol^{-1} cm^{-1}) 340 (2960); Λ_m(freshly prepared solution in DMF) = 50 mol^{-1} cm^2 Ω^{-1} (c.f. 65−90 Ω^{-1} mol^{-1} cm^{-1} for a 1:1 electrolyte in DMF);[55] FAB mass spectrum *m*/*z* 636 $[Ni_2(L1)(SCN)]^+$; 578 $[Ni_2(L1)]^+$; μ = 2.8 BM.

$[Ni_2L2(NCS)_2]$ (5): A colourless MeCN solution (4 cm^3) of sodium thiocyanate (0.0128 g, 0.154 mmol) was layered on top of a deep red MeCN solution (1 cm^3) of **2b** (0.060 g, 0.071 mmol). On standing, red-black crystals of **5** formed, along with a brown precipitate, leaving a light yellow solution. The crystals were physically separated from the powder, washed with MeCN and dried in vacuo (0.009 g, 19%). (Found: C 47.2, H 3.6, N 13.0, S 19.7. $C_{26}H_{26}N_6Ni_2S_4$ (**5**) requires C 46.8, H 3.9, N 12.6, S 19.2%); $\tilde{\nu}/cm^{-1}$ (KBr disk, inter alia) 2075, 1621; λ_{max}/nm (MeCN) (ε/L mol^{-1} cm^{-1}) 335 (2820); Λ_m(DMF) = 70 Ω^{-1} mol^{-1} cm^{-1} (c.f. 65−90 Ω^{-1} mol^{-1} cm^{-1} for a 1:1 electrolyte in DMF);[55] FAB mass spectrum *m*/*z* 550 $[Ni_2L2]^+$.

$[Ni_2L'(MeCN)_4](ClO_4)_2$ (6): $[Ni_2L'Cl_2]$ (0.120 g, 0.17 mmol) was dissolved in a 1:1 mixture of MeCN:water (10 cm^3). To this green solution was added $AgClO_4$ (0.072 g, 0.35 mmol) and the resulting off-white precipitate filtered off.[28] Overnight a dark green crystalline solid formed in the filtrate. This was collected and recrystallised from MeCN by vapour diffusion of diethyl ether to give **6** as large dark green blocks (0.115 g, 76%). (Found: C 43.3, H 4.6, N 12.5, $C_{32}H_{38}Cl_2N_8Ni_2O_{10}$ requires C 43.5, H 4.3, N 12.7%); $\tilde{\nu}/cm^{-1}$ (KBr disk, inter alia) 1639, 1083, 625; λ_{max}/nm (MeCN) (ε/L^{-1} mol^{-1} cm^{-1}) 375 (12800); Λ_m(DMF) = 180 mol^{-1} cm^2 Ω^{-1} (c.f. 130−170 Ω^{-1} mol^{-1} cm^{-1} for a 2:1 electrolyte in DMF);[55] FAB mass spectrum *m*/*z* 617 $[Ni_2(L')(ClO_4)]^+$; 518 $[Ni_2L']^+$.

X-ray Crystallography: Data were collected, on **1a** at 153 K with a Siemens P4 four circle diffractometer and on **5** and **6** at 158 K with a Bruker SMART diffractometer, using graphite-monochromated Mo-*K*α radiation (λ = 0.71013 Å). The data were corrected for Lorentz and polarisation effects and empirical absorption corrections were applied. Hydrogen atoms were inserted at calculated positions and rode on the atoms to which they are attached (including isotropic thermal parameters which were equal to 1.2 times the equivalent isotropic displacement parameter for the attached non-hydrogen atom).

Crystal data for **1a** ($C_{28}H_{33.5}Cl_2N_5Ni_2O_{8.25}S_2$): M_r = 412.3, red block, 0.50 × 0.50 × 0.40 mm, triclinic, space group *P*-1, *a* = 18.174(4), *b* = 18.997(9), *c* = 23.121(8) Å, α = 70.56(3), β = 69.58(3), γ = 77.78(2)°, *V* = 7013(4) $Å^3$, *Z* = 8, μ = 1.40 mm^{-1}, ρ_{calc} = 1.562 g cm^{-3}. A total of 18709 reflections were collected in the range 4 < 2θ < 45°, and the 18013 independent reflections were used in the structural analysis after a semi-empirical absorption correction had been applied (T_{min} = 0.41, T_{max} = 0.50). The structure, four independent macrocyclic complexes in the asymmetric unit, was solved by direct methods (SHELXS-86)[56][57] and refined against all F^2 data (SHELXL-93)[58] to *R1* = 0.083 [for 10954 $F > 4\sigma(F)$; *wR2* = 0.239 and GOF = 1.04 for all 18013 F^2; 1370 parameters; all Ni, S/N/alkyl-C atoms of the macrocycles, O/N/Cl of the full occupancy solvents and perchlorates, Cl(8) and Cl(9) of the partial occupancy perchlorates, anisotropic; 2 (of 8) perchlorates and 2 (of 4) acetonitriles disordered; +1.77/−1.11 e$Å^{-3}$].

Crystal data for **4** · 2 MeCN ($C_{32}H_{36}N_8Ni_2S_4$): M_r = 778.4, red-black rectangular plate, 0.80 × 0.20 × 0.03 mm, triclinic, space group *P*-1, *a* = 10.134(2), *b* = 11.273(2), *c* = 16.112(4) Å, α = 83.957(3), β = 82.082(3), γ = 73.049(3)°, *V* = 1739.7(6) $Å^3$, *Z* = 2, μ = 1.36 mm^{-1}, ρ_{calc} = 1.486 g cm^{-3}. A total of 11118 reflections were collected in the range 5 < 2θ < 53°, and the 6468 independent reflections were used in the structural analysis after a semi-empirical absorption correction had been applied (T_{min} = 0.43, T_{max} = 1.00). The structure was solved by direct methods (SHELXS-97)[56][57] and refined against all F^2 data (SHELXL-97)[58] to *R1* = 0.0446 [for 4250 $F > 4\sigma(F)$; *wR2* = 0.1220 and GOF = 0.92 for all 6468 F^2; 419 parameters; all non-hydrogen atoms anisotropic; +0.79/−0.61 e$Å^{-3}$].

Crystal data for **5** · MeCN ($C_{28}H_{29}N_7Ni_2S_4$): M_r = 709.2, red-black rectangular plate, 0.60 × 0.30 × 0.03 mm, monoclinic, space group $P2_1/c$, *a* = 12.466(5), *b* = 14.267(5), *c* = 17.226(6) Å, β = 93.792(5)°, *V* = 3056.9(19) $Å^3$, *Z* = 4, μ = 1.54 mm^{-1}, ρ_{calc} = 1.541 g cm^{-3}. A total of 32103 reflections were collected in the range 5 < 2θ < 53°, and the 6244 independent reflections were used in the structural analysis after a semi-empirical absorption correction had been applied (T_{min} = 0.76, T_{max} = 1.00). The structure was solved by direct methods (SHELXS-97)[56][57] and refined against all F^2 data (SHELXL-97)[58] to *R1* = 0.0328 [for 3601 $F > 4\sigma(F)$; *wR2* = 0.0612 and GOF = 0.79 for all 6244 F^2; 373 parameters; all non-hydrogen atoms anisotropic; +0.51/−0.49 e$Å^{-3}$].

Crystallographic data (excluding structure factors) for the structures reported in this paper have been deposited with the Cambridge Crystallographic Data Centre as supplementary publication numbers CCDC-125078, CCDC-125079 and CCDC-125080. Copies of the data can be obtained free of charge on application to CCDC, 12 Union Road, Cambridge CB2 1EZ, UK [Fax: (+44) 1223/336-033; E-mail: deposit@ccdc.cam.ac.uk].

Acknowledgments

This work was supported by grants from the University of Otago. We are grateful to Professor W. T. Robinson and Dr. J. Wikaira (University of Canterbury) for the X-ray data collections, B. M. Clark (University of Canterbury) for the FAB mass spectra, Dr. M. Thomas (University of Otago) for obtaining the NMR spectra, and to V. Camplin and R. Cooke (University of Otago) for their help. The help and advice given to us by Professor A. McAuley (University of Victoria), particularly regarding the interpretation of the EPR spectra run by CB and SS, is greatly appreciated. We thank Dr. E. Bothe and Professor K. Wieghardt (MPI für Strahlenchemie) for providing us with details of their spectroelectrochemical cell design and gratefully acknowledge the glass blowing skills of J. Wells (University of Otago) which allowed construction of this cell.

[1] R. Cammack, *Nature* **1999**, *397*, 214.
[2] M. Frey, *Struct. Bond.* **1998**, *90*, 97.
[3] J. C. Fontecilla-Camps, *Struct. Bond.* **1998**, *91*, 1.
[4] A. Volbeda, M. H. Charon, C. Piras, E. C. Hatchikian, M. Frey, J. C. Fontecilla-Camps, *Nature* **1995**, *373*, 580.
[5] M. A. Halcrow, G. Christou, *Chem. Rev.* **1994**, *94*, 2421.
[6] G. Musie, P. J. Farmer, T. Tuntulani, J. H. Reibenspies, M. Y. Darensbourg, *Inorg. Chem.* **1996**, *35*, 2176.
[7] C. H. Lai, J. H. Reibenspies, M. Y. Darensbourg, *Angew. Chem.* **1996**, 108, 2551; *Angew. Chem. Int. Ed. Engl.* **1996**, *35*, 2390.
[8] T. Beissel, F. Birkelbach, E. Bill, T. Glaser, F. Kesting, C. Krebs, T. Weyhermuller, K. Wieghardt, C. Butzlaff, A. X. Trautwein, *J. Am. Chem. Soc.* **1996**, *118*, 12376.
[9] T. Glaser, F. Kersting, T. Beissel, E. Bill, T. Weyhermueller, W. Meyer-Klaucke, K. Wieghardt, *Inorg. Chem.* **1999**, *38*, 722.
[10] P. Illiopoulos, K. S. Murray, R. Robson, J. Wilson, G. A. Williams, *J. Chem. Soc., Dalton Trans.* **1987**, 1585.
[11] A. M. Bond, M. Haga, I. S. Creece, R. Robson, J. C. Wilson, *Inorg. Chem.* **1988**, *27*, 712.
[12] A. M. Bond, M. Haga, I. S. Creece, R. Robson, J. C. Wilson, *Inorg. Chem.* **1989**, *28*, 559.
[13] B. F. Hoskins, C. J. McKenzie, R. Robson, Z. R. Lu, *J. Chem. Soc., Dalton Trans.* **1990**, 2637.
[14] S. Brooker, P. D. Croucher, *J. Chem. Soc., Chem. Commun.* **1995**, 2075.
[15] S. Brooker, P. D. Croucher, *J. Chem. Soc., Chem. Commun.* **1995**, 1493.
[16] S. Brooker, P. D. Croucher, F. M. Roxburgh, *J. Chem. Soc., Dalton Trans.* **1996**, 3031.
[17] S. Brooker, T. C. Davidson, *Chem. Commun.* **1997**, 2007.
[18] S. Brooker, P. D. Croucher, *Chem. Commun.* **1997**, 459.
[19] S. Brooker, P. D. Croucher, T. C. Davidson, G. S. Dunbar, A. J. McQuillan, G. B. Jameson, *Chem. Commun.* **1998**, 2131.
[20] A. J. Atkins, A. J. Blake, M. Schroder, *J. Chem. Soc., Chem. Commun.* **1993**, 1662.
[21] A. J. Atkins, D. Black, A. J. Blake, A. Marin-Becerra, S. Parsons, L. Ruiz-Ramirez, M. Schroder, *Chem. Commun.* **1996**, 457.
[22] N. D. J. Branscombe, A. J. Blake, A. Marin-Becerra, W. S. Li, S. Parsons, L. Ruiz-Ramirez, M. Schroder, *Chem. Commun.* **1996**, 2573.
[23] A. Christensen, H. S. Jensen, V. McKee, C. J. McKenzie, M. Munch, *Inorg. Chem.* **1997**, *36*, 6080.
[24] P. E. Kruger, V. McKee, *Chem. Commun.* **1997**, 1341.
[25] G. A. Lawrance, M. Maeder, T. M. Manning, M. A. O′Leary, B. W. Skelton, A. H. White, *J. Chem. Soc., Dalton Trans.* **1990**, 2491.
[26] N. F. Curtis, *J. Chem. Soc.* **1965**, *169*, 924.
[27] N. H. Pilkington, R. Robson, *Aust. J. Chem.* **1970**, *23*, 2237.
[28] H. Okawa, private communication.
[29] K. Nakamoto, *Infrared and Raman Spectra of Inorganic and Coordination Compounds, Wiley, New York*, **1997**, *Part B*, 53.
[30] H. Frydendahl, H. Toftlund, J. Becher, J. C. Dutton, K. S. Murray, L. F. Taylor, O. P. Anderson, E. R. T. Tiekink, *Inorg. Chem.* **1995**, *34*, 4467.
[31] I. G. Dance, *Polyhedron* **1986**, *5*, 1037.
[32] J. R. Dilworth, J. Hu, *Adv. Inorg. Chem.* **1993**, *40*, 411.
[33] G. Aullon, G. Ujaque, A. Lledos, S. Alvarez, *Chem. Eur. J.* **1999**, *5*, 1391.
[34] C. A. Hunter, *Chem. Soc. Rev.* **1994**, *23*, 101.
[35] M. D. Glick, R. L. Lintvedt, T. J. Anderson, J. L. Mack, *Inorg. Chem.* **1976**, *15*, 2258.
[36] M. P. Suh, *Adv. Inorg. Chem.* **1997**, *44*, 93.
[37] A. McAuley, K. Beveridge, S. Subramanian, T. W. Whitcombe, *J. Chem. Soc., Dalton Trans.* **1991**, 1821.
[38] X. Chen, S. Zhan, C. Hu, Q. Meng, J. Shun, *Inorg. Chim. Acta.* **1997**, *260*, 95.
[39] B. Kersting, G. Steinfeld, J. Hausmann, *Eur. J. Inorg. Chem.* **1999**, 179.
[40] B. Kersting, D. Siebert, *Inorg. Chem.* **1998**, *37*, 3820.
[41] B. Kersting, *Eur. J. Inorg. Chem.* **1998**, 1071.
[42] B. Kersting, G. Steinfeld, J. Hausmann, *Eur. J. Inorg. Chem.* **1999**, 179.
[43] B. Kersting, D. Siebert, *Eur. J. Inorg. Chem.* **1999**, 189.
[44] T. J. Kemp (Ed.), *Southampton Electrochemistry Group: Instrumental Methods in Electrochemistry*, Ellis Horwood Ltd, Chichester, **1985**.
[45] H. J. Kruger, R. H. Holm, *Inorg. Chem.* **1987**, *26*, 3645.
[46] Y. Aratake, M. Ohba, H. Sakiyama, M. Tadokoro, N. Matsumoto, H. Okawa, *Inorg. Chim. Acta.* **1993**, *212*, 183.
[47] K. K. Nanda, R. Das, K. Venkatsubramanian, P. Paul, K. Nag, *J. Chem. Soc., Dalton Trans.* **1993**, 2515.
[48] K. K. Nanda, A. W. Addison, N. Paterson, E. Sinn, L. K. Thompson, U. Sakaguchi, *Inorg. Chem.* **1998**, *37*, 1028.
[49] D. H. Busch, E. S. Gore, F. V. Lovecchio, *J. Am. Chem. Soc.* **1974**, *96*, 3109.
[50] T. Yamamura, M. Tadokoro, K. Tanaka, R. Kuroda, *Bull. Chem. Soc. Jpn.* **1993**, *66*, 1984.
[51] A. G. Lappin, A. McAuley, *Adv. Inorg. Chem.* **1988**, *32*, 241.
[52] P. Delahay, C. W. Tobias, *Advances in Electrochemistry and Electrochemical Engineering*, Wiley, New York, **1970**, *7*, 77.
[53] R. I. Haines, A. McAuley, *Coord. Chem. Rev.* **1981**, *39*, 77.
[54] M. B. Robin, P. Day, *Adv. Inorg. Chem. Radiochem.* **1967**, *10*, 247.
[55] W. J. Geary, *Coord. Chem. Rev.* **1971**, *7*, 81.
[56] G. M. Sheldrick, *Acta Crystallogr., Sect. A* **1990**, *46*, 467.
[57] G. M. Sheldrick, *Methods Enzymol.* **1997**, *276*, 628.
[58] G. M. Sheldrick, T. R. Schneider, *Methods Enzymol.* **1997**, *277*, 319.

Received August 17, 1999
[I99304]